

Perceptually Transparent Binaural Auralization of Simulated Sound Fields

Jens Ahrens, jens.ahrens@chalmers.se

December 9, 2024

Abstract

Contrary to geometric acoustics-based simulations where the spatial information is available in a tangible form, it is not straightforward to auralize wave-based simulations. A variety of methods have been proposed that compute the ear signals of a virtual listener with known head-related transfer functions from sampling either the sound pressure or the particle velocity (or both) of the simulated sound field. The available perceptual evaluation results of such methods are not comprehensive so that it is unclear what number and arrangement of sampling points is required for achieving perceptually transparent auralization, i.e. for achieving an auralization that is perceptually indistinguishable from the ground truth. This article presents a perceptual evaluation of the most common binaural auralization methods with and without intermediate ambisonic representation of volumetrically sampled sound pressure or sound pressure and particle velocity sampled on spherical or cubical surfaces. Our results confirm that perceptually transparent auralization is possible if sound pressure and particle velocity are available at 289 sampling points on a spherical surface grid. Other grid geometries require considerably more points. All tested methods are available open source in the Chalmers Auralization Toolbox that accompanies this article.

1 INTRODUCTION

Wave-based methods like Finite Element Method (FEM), Boundary Element Method (BEM), and Finite-Difference Time-Domain (FDTD) are becoming increasingly popular for room acoustic simulations, and simulations over the entire audible frequency range are possible. Contrary to geometric acoustics-based simulations where the spatial information is available in a tangible form in terms of, for example, incidence directions and spectral fingerprints of reflections [1, 2, 3, 4], it is not straightforward to auralize wave-based simulations, and a vari-

ety of approaches have been proposed.

The output of wave-based simulations may be termed a *virtual sound field*, and the format that the output of any wave-based simulation method can be converted to is the sound pressure and/or particle velocity at a set of observation points, which we term *sampling points* or *sampling nodes*. Those auralization approaches that require sampling of a virtual sound field on an infinitesimal portion of space around the notional receiver point to be auralised may be termed *local*. Examples are [5], which uses virtual microphones for obtaining a spherical harmonic (SH) representation of the sampled sound field, and [6, 7], which obtain SH representations via higher-order spatial derivatives. Local approaches require higher-order time integration, which exhibits the inconvenience that it produces a DC drift that is difficult to tame [8].

Non-local approaches include [9], which obtains SH coefficients by numerically evaluating a boundary integral of pressure and velocity, and [10, 11, 12, 13], which sample a portion of space volumetrically.

The method from [9] is directly integrated in the BEM framework, and it is difficult to anticipate what it will take to make it work accurately in other frameworks. It is also unclear at this point in how far the current limitations of the local approaches can be overcome so that we limit our considerations to methods like [10, 11, 12] that work based sampling the virtual sound field in a portion of space of moderate size.

Some of the methods mentioned above work solely based on the sampled sound pressure of the simulated field, which can lead to ill-conditioning of the problem. The methods that we consider here are closely related to binaural rendering of microphone array recordings in the literature where this ill-conditioning is well known [14, 15]. The set of sampling nodes in the present case can be interpreted as a virtual microphone array. The main difference is that, contrary to real microphones, the sampling nodes are ideal and their number and placement are virtually

unrestricted. Combining pressure and pressure gradient can greatly improve the conditioning of the problem [16, 14]. One incarnation of this combination are (virtual or actual) microphones with cardioid directivity [15, 17], which are a promising solution to the present problem [18].

We want to emphasize that our work does not evaluate acoustical simulations themselves. Our purpose is to investigate how non-geometrical acoustics simulations can be auralized binaurally, i.e. how to most favorably compute signals from the output of the simulation that would arise at a listener’s ears if the listener were exposed to the simulated sound field. As it is likely that it will not be possible to achieve that the output of the auralization is numerically identical to the ground truth, we seek for *perceptually transparent* auralization, i.e. auralization that is perceptually indistinguishable from the ground truth.

Our investigation is not based on the output of an actual simulation framework. We rather use a representation of room acoustic responses from which we can compute both a binaural ground truth signal as well as sampled sound field data the auralization of which we evaluate against the binaural ground truth. Previous perceptual evaluations of auralization of non-geometric acoustics simulations used auralization of limited scope or frequency range (or both) [13, 19, 20]. The potential for general perceptual transparency is therefore unclear.

The auralization solution that we seek in this manuscript is intended to be as general as possible, which means that we only consider solutions that 1) do not make assumptions on the sound field that is to be auralized, and that 2) can work on running signals.

The motivation for 1) is that the auralization is desired to be applicable to any simulated sound field. There are methods that were originally proposed in the field of auralization of microphone array measurements of room impulse responses such as [21, 22] that parameterize the sound field, for example into direct and diffuse components. This can indeed provide a benefit over non-parametric methods, especially when the number of sampling nodes is small. Yet, there is uncertainty in the output from parametric methods if non-standard sound fields are considered such as sound fields outdoors, in small compartments like in car cabins where it is not straightforward to differentiate direct sound from early reflections, or if occlusion of the direct sound occurs.

Linear and time-invariant (LTI) sound field simulations can be expressed in terms of impulse responses. While this is likely to be the most common application area of auralization today, we still formulate requirement 2) so that also dynamic scenarios and scenarios

that comprise nonlinearities such simulations of electroacoustic systems can be handled. Parametric rendering methods have also been proposed for running signals [23, 24]. We exclude those from the present investigation for the reasons stated above.

For convenience, our investigation is performed based on simulated room impulse responses. This does not limit the generalizability of the results as all methods can be straightforwardly applied to running signals without modification.

2 Auralization Framework

What is common to all auralization methods that we consider here is that the auralization itself is modelled as an LTI system and is represented by a set of impulse responses. The set of impulse responses essentially represents the multiple-input and multiple-output (MIMO) transfer path from the sampling nodes to the ears of the listener. Refer to Fig. 1 for an illustration. The transfer path therefore comprises the head-related transfer function (HRTFs) of the listener as well as their head orientation. Once the impulse responses have been computed, carrying out the auralization consists in performing the required convolutions. This process is often termed *rendering* in spatial audio. The result of the rendering is the ear signals that would arise at the listener’s ears if they were exposed to the virtual sound field with a given head orientation.

The available methods may be divided in two categories: Methods that we term here *direct methods* obtain the binaural output signals directly from the signals at the sampling nodes. Methods that we term here *ambisonic methods* produce a representation of the sampled sound field in terms of spherical harmonic basis functions (SHs). This representation is also referred to as ambisonic representation and can be rendered binaurally or using a loudspeaker array [25]. The advantage of the ambisonic methods is that the problem of auralization is decomposed into two independent stages that can be optimized separately. From a purely practical perspective, head-tracked rendering of the ambisonic representation can be carried out straightforwardly by applying rotation operations on either the ambisonic sound field or the ambisonic HRTF representation. The application of head tracking on the rendering side in direct auralization requires computing the auralization separately for each possible head orientation of the listener, which can be a substantial computational burden.

The following subsections outline the signal processing in the auralization methods that we investi-

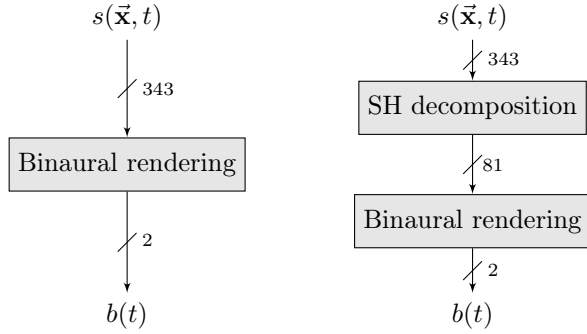


Figure 1: Block diagram of the signal processing pipeline for direct auralization (left) and ambisonic auralization (right). $s(\vec{x}, t)$ are signals at the sampling nodes \vec{x} and $b(t)$ is the binaural output. Each of the gray blocks represents a MIMO convolution. In these examples, 343 sampling nodes are assumed as well as an ambisonic representation of order $N = 8$, which produces an ambisonic signal with 81 channels. In either case, the binaural rendering stage takes the instantaneous head orientation of the listener into account.

gated. We were required to make a significant number of decisions in the choice of implementation details because the literature provides primarily concepts rather than comprehensive validated solutions. Our choices were based on extensive experimentation, and there were a number of situations where it was not obvious which candidate was better than the others, in which case we always chose the simplest option. For the purpose of reproducibility, we provide all our implementations in the Chalmers Auralization Toolbox [26, 27]. As we will discuss below, we extended the available methods such that both ambisonic auralization and direct auralization can be carried out based on cubical volumetric sampling (CV) and based on spherical and cubical surface sampling (SS and CS) of the virtual sound field. Fig. 2 depicts examples for all three types of sampling grids.

While all investigated methods are formulated in frequency domain, it appears more flexible if the auralization is carried out in practice via block-wise processing of time-domain signals. This is also how the Chalmers Auralization Toolbox performs it. We highlight here that this presents challenges regarding the implementation for a variety of reasons. For example, the DC part of a given spectral representation can be undefined, or time aliasing can occur, which are both challenges that do not occur in pure frequency-domain considerations. The discussion of the implementation details is beyond the scope of this article,

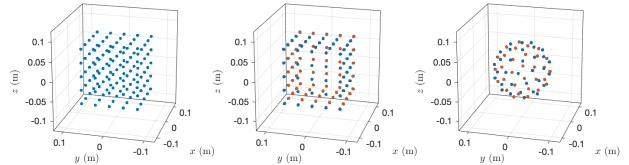


Figure 2: The employed sampling grids. Left: Volumetric cube (125 nodes). Middle: Cubical surface grid (98 double nodes). Right: Spherical surface grid (64 double nodes). With the surface grids, blue color indicates a pressure node, and orange color indicates a coincident velocity node. The diameter of the spherical grid and the edge length of the cubical grids are 140 mm.

and we refer the reader to the documentation and the code of the Chalmers Auralization Toolbox.

2.1 The Ambisonic Methods

The ambisonic methods that we investigate are based on [12], which is formulated for volumetrically sampled sound pressure fields and may be considered an extension of [10]. The SH representation is obtained via inversion of a matrix of the SH basis terms. Contrary to [12], we use a singular value decomposition (SVD) [28] that is regularized by limiting the dynamic range of the singular values to regularize the matrix inversion instead of soft-clipping of the matrix elements followed by an unregularized pseudo inverse.

Volumetric sampling may be inefficient in that it may require unnecessarily many sampling points to yield a well-conditioned problem. The Kirchhoff-Helmholtz integral [29] demonstrates that the sound pressure field inside a source-free domain is uniquely described by the sound pressure $S(\vec{x}, \omega)$ and normal sound pressure gradient $\frac{\partial}{\partial \mathbf{n}} S(\vec{x}, \omega)$ distributions along the simply connected surface that encloses the domain. It is proven in [16, p. 207] that a weighted sum $S(\vec{x}, \omega) + \gamma \frac{\partial}{\partial \mathbf{n}} S(\vec{x}, \omega)$ uniquely defines the sound pressure inside the volume that is enclosed by the surface so long as $\text{Im}\{\gamma\} \neq 0$. Choosing $\gamma = 1/(i\frac{\omega}{c})$ fulfills the uniqueness criterion and is a particularly convenient choice as it assures that pressure and gradient are added with similar magnitudes. It also allows for the weighted sum to be interpreted as a virtual sensor with (far-field) cardioid directivity, which connects our formulation well to the literature on microphone arrays [15, 17]. This enables the employment of surface sampling grids, which may potentially be more efficient than volumetric ones.

The sound pressure gradient can be straightforwardly computed from the particle velocity [30], which number simulation methods provide straight-

forwardly. If the particle velocity is not available, then it can be obtained from sampling the sound pressure along two surfaces that are much closer to each other than the wavelength. We confirmed through informal listening that the binaural output signals produced from a double pressure layer are perceptually identical to the binaural output signals produced from pressure and velocity along one surface layer so long as the distance between layers is not larger than 5 mm.

Extending [12] to spherical surface grids with radially outward-facing cardioid sensors is straightforward given the literature on spherical microphone arrays [15]. The mathematical details are provided in the documentation of the Chalmers Auralization Toolbox. As to our awareness, cardioid sensors have only been used along circular and spherical contours for performing SH sound field decomposition. This is unfortunate as some wave-based simulation methods such as FDTD can employ Cartesian sampling schemes that would require interpolation to realize a spherical sampling grid. To bridge this gap, we extended the method from [12] to arbitrary simply connected surface grids with normally outward-facing cardioid sensors. We included cubical surface grids into the present investigation. This solution was not available in the literature and is an original contribution by the authors. The mathematics behind it is not straightforward, and we refer the reader to the documentation of the Chalmers Auralization Toolbox for details.

There are two main sources for systematic inaccuracies in ambisonic auralization: 1) Spatial aliasing due to the discretization of the sampled sound field and 2) order truncation of the SH representation of the sound field (and consequently of the HRTFs). Spatial aliasing typically increases the energy at high frequencies, and order truncation decreases or increases it depending on the incidence direction [31]. Anticipating the interaction between the two is not straightforward. Contrary to the original formulations of ambisonic auralization [10, 12], we employ a magnitude least-squares (MagLS) SH representation of the HRTFs [32], which essentially eliminates the effect of the order truncation on the HRTFs. Fig. 3 illustrates this exemplarily for an SH order of $N = 4$. The effect of spatial aliasing and order limitation on the distribution of the energy over the frequency axis in the decomposed sound field is hardly dependent on the incidence direction of the sound field. We therefore equalize it by computing a global minimum-phase filter that minimises the deviation of the binaural output from the ground truth averaged over many sound incidence directions. This equalization filter is only effective at high frequencies above several kHz. Re-

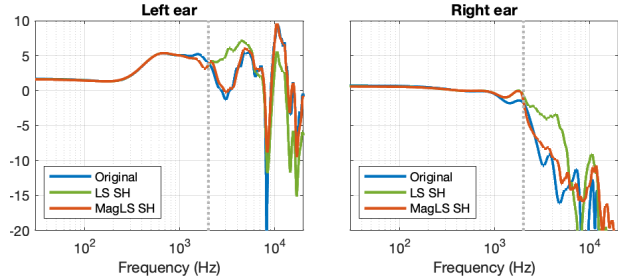


Figure 3: The employed HRTFs (blue line) as well as their SH representations for sound incidence from the left computed from a 4th-order SH decomposition using the conventional least-squares (LS) fit of SH coefficients (green line) as well as using a MagLS fit (orange line). The gray dotted line indicates the frequency below which LS and above which MagLS was used to compute the SH coefficients in the case that is labelled MagLS.

calling that HRTFs are defined as the acoustic ear signals due to a plane wave in free-field conditions makes sampled plane waves and HRTFs a convenient set of input/output data based on which this equalization filter can be computed.

Independent of the sampling grid, the ambisonic methods produce an SH representation of the sampled sound field. The binaural rendering of these is well established and detailed, for example, in [33].

2.2 The Direct Methods

The direct auralization methods are based on [11]. The auralization is modelled as a MIMO system the input to which is the sampled sound field data. The output are the left and right ear signals. The set of filters that represent the transfer path between the input and the output are computed through a least-squares (LS) fit on sample data. Recalling again that HRTFs are defined as the acoustic ear signals due to a plane wave in free-field conditions makes sampled plane waves and HRTFs a convenient set of input/output data for computing the LS solution. The original method was demonstrated for volumetrically sampled sound pressure. Applying it to spherical and cubical surface sampled data does not require any modifications.

Like any other method, direct auralization suffers from spatial aliasing (above approx. 8 kHz in Fig. 4). The LS solution can exhibit large errors in the frequency range where spatial aliasing occurs. We found that the solution is perceptually more favorable if the LS solution is replaced with a MagLS solution in the frequency range where the spatial aliasing occurs.

Our implementation corresponds to what is termed end-to-end MagLS, variant 2, in [34].

3 Grid Parameters

Choosing the parameters for a grid with a given number of nodes is a compromise: A grid with large dimensions is desired for being able to resolve spatial information at low frequencies. Keeping the spatial aliasing frequency, i.e. the frequency above which spatial aliasing occurs, high requires a small spacing between the nodes. It was demonstrated in [31] that high SH order spatial information at low frequencies in the sound field does not reach the ear of the listener because it is suppressed by the directivity of the ears. The sampling grid can therefore be small compared to the wavelength, which is favorable as this produces a high spatial aliasing frequency. We verified using the approach from [31] that a diameter or edge length of 0.14 m is the smallest size that avoids compromises in the binaural output signals due to the required regularization. We chose it for all grids. We could not find a noteworthy benefit in choosing a different grid size for any of the investigated configurations.

Solutions for optimal placement of sampling points in a volume or on a surface contour for sound field decomposition have been proposed in the literature [35, 36, 37]. These have only been demonstrated in narrow frequency ranges. It is unclear how they can be extended to the entire audible frequency range that is of interest here. We therefore only consider evenly sampled grids in this article. This means that only certain numbers of sampling nodes are possible for cubical volumetric and cubical surface grids, see Tab. 2. We selected the layout for spherical surface grids from Fliege grids [38] with comparable numbers of nodes.

Tab. 1 lists all investigated grid layouts. We found that it was not useful to use cubical volumetric grids with an SH order of higher than $N = 18$. Example binaural data are provided in Fig. 4. The different parameters produce primarily differences only at high frequencies where spatial aliasing limits the accuracy.

4 Computation of the Ground Truth

Validation of the perceptual transparency of the auralization requires comparing the auralization to the ground truth ear signals. Anechoic conditions are straightforward given that HRTFs are defined as the acoustic ear signals due to a plane wave in free-field conditions. We therefore used spatially sampled plane

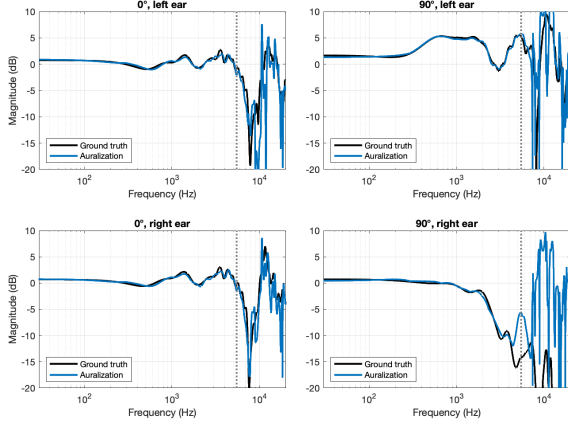
$L_{\text{cub. vol.}}$	$L_{\text{cub. surf.}}$	$L_{\text{sph. surf.}}$
27 (2)		
64 (3)	26 (3)	25 (3)
125 (5)	56 (5)	64 (6)
216 (7)	98 (7)	100 (8)
343 (11)	152 (9)	169 (11)
512 (15)	218 (11)	225 (13)
	296 (13)	289 (15)
729 (18)	386 (15)	400 (18)
1000 (18)	488 (17)	484 (20)
1331 (18)		
1728 (18)		
2197 (18)		

Table 1: Number L of data points for the different grids. See Fig. 2 for examples. The figure in parentheses states the maximum SH order N that can be extracted from the grid. Note that L for the surface grids refers to the number of pairs of data points. Grid with approximately the same number of data points are stated in the same row. The cubical grids have an edge length of 0.14 m and the spherical grids have a diameter of 0.14 m.

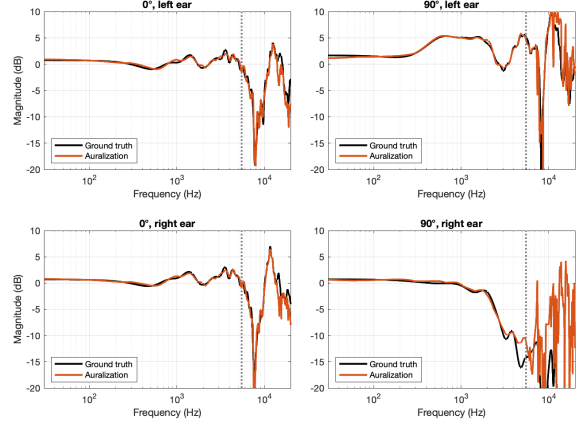
waves as the input to the auralization and the HRTFs as the ground truth in this setting.

Reverberant conditions are less straightforward in that no wave-based simulation method is free of systematic errors, and it is not straightforward how to compute the ground truth ear signals. Simpler room acoustic simulation methods like the image source method allow for computing a ground truth, but the resulting reverberation can sound unnatural.

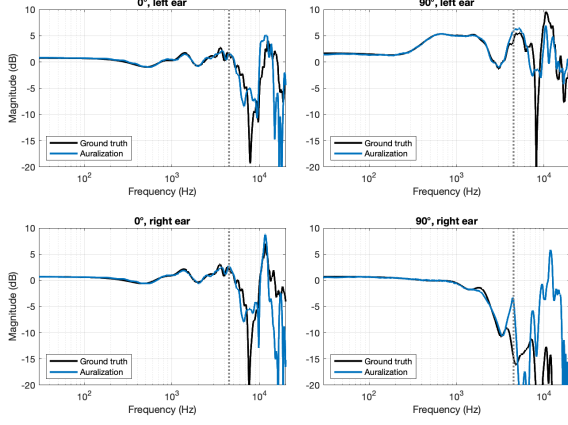
We therefore chose the following procedure: The spatial decomposition method (SDM) [39] produces a representation of a room impulse response in terms of the pressure impulse response as well as an incidence direction for each digital sample of the pressure impulse response. A binaural representation of the room impulse response can be obtained by assigning the HRTF that corresponds to the incidence direction of a given digital sample to that digital sample and superposing the weighted HRTFs for all digital samples. This binaural representation has been shown to be perceptually slightly different from the actual binaural room response. We chose it for the present purpose because it was confirmed by different authors that the perceptual result is highly plausible [40, 41]. The input data to the auralization can be computed from the SDM data by assigning plane waves with appropriate incidence directions instead of HRTFs to each digital sample. Fig. 5 illustrates the concept. An implementation is available at [42].



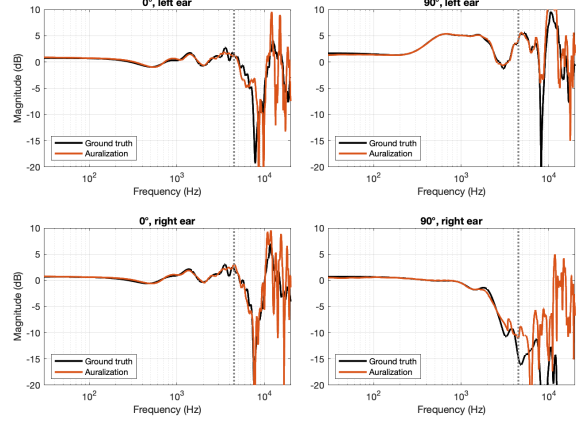
(a) Cubical volume, $L_{\text{cub. vol.}} = 343$, $N = 11$



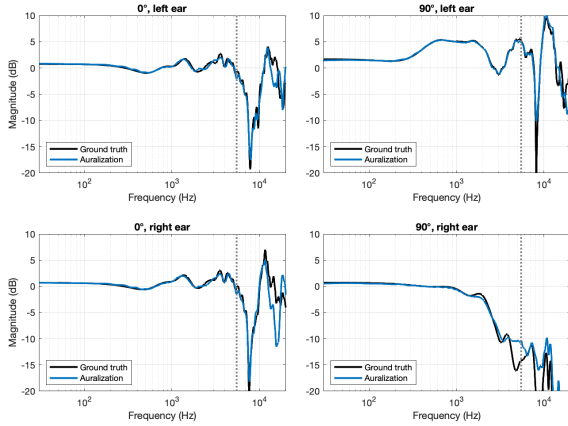
(b) Cubical volume, $L_{\text{cub. vol.}} = 343$



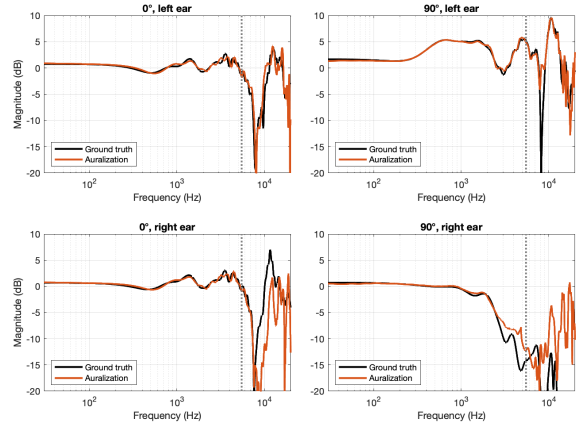
(c) Cubical surface, $L_{\text{cub. surf.}} = 152$, $N = 9$



(d) Cubical surface, $L_{\text{cub. surf.}} = 152$



(e) Spherical surface, $L_{\text{sph. surf.}} = 169$, $N = 11$



(f) Spherical surface, $L_{\text{sph. surf.}} = 169$

Figure 4: Example anechoic binaural data for each combination of grid and method (Left column: ambisonic auralization. Right column: direct auralization). The binaural output is due to a plane wave with incidence from straight ahead or from 90° to the left. The ground truth is the HRTF corresponding to the given incidence direction. The vertical dotted lines indicate above what frequency MagLS-HRTFs are employed (ambisonic methods) or the eMagLS solution is employed (direct methods). All data were computed by performing the auralization on the time-domain signals.

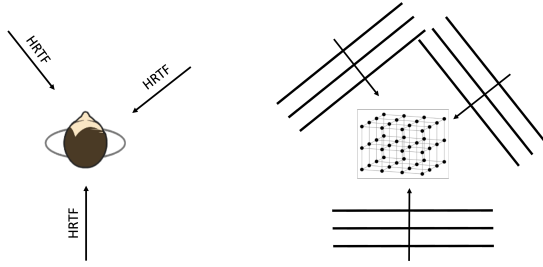


Figure 5: Illustration of the computation of the ground truth binaural signal (left) and the sampled sound field data (right) based on SDM data as performed for the reverberant condition.

5 Perceptual Experiment

The experiment used a transformed two-up/one-down staircase procedure to determine the threshold of detectability of a difference between the stimulus and the ground truth [43]. The subjects were presented with a graphical interface with three buttons in each trial. Two of the buttons played identical signals (reference or stimulus), and the third one played the corresponding other signal. The assignment of the buttons was random. The subject’s task was to report via a button click which of the three stimuli sounded different from the other two, and the subjects could listen to the stimuli as many times as they wanted. The experiment started with the lowest number of sampling points for each combination of auralization method, grid parameters, and room data. The number of sampling points based on which the stimulus was computed (and thereby the numerical accuracy of the stimulus) increased after two consecutive correct answers and decreased after each incorrect answer (2-up-1-down). The adaptation stopped after six reversals of the direction. A wrong answer for the lowest number of sampling points is also counted as a reversal.

The experiment was carried out in two sessions for each subject with three adaptations per session. Each session started with a training of one complete adaptation using stimuli that were computed based on different parameter choices in the signal processing compared to those that occurred in the experiment. The order of the different tested parameter sets was randomized for each subject.

The experiment was carried out with head tracking along the azimuth. Each condition was represented by a pre-computed set of binaural impulse responses for different azimuth head orientations with a resolution of 1° that were convolved with the input signal. We discuss the choice of input signal below. The graphi-

cal interface was implemented in MATLAB¹, the audio playback and routing in Pure Data², head tracking was performed with a Supperware Head Tacker³, and realtime convolution was carried out by SoundScape Renderer (SSR) [44].

It was confirmed in [45, 46] and other locations in the literature that lateral sound incidence is the most revealing one for detecting perceptual differences between reference and stimulus. This is presumably because the signal at the contralateral ear exhibits comparatively low energy so that artifacts become perceptually more prominent. The artifacts at the contralateral ear are even numerically prominent in Fig. 4. To account for this, the graphical interface comprised a button with which the subjects could switch between hearing the virtual sound source from the nominal directions of straight ahead and from 90° to the right so that they would have an efficient means of verifying different incidence directions without having to turn the head excessively.

Experiments that we conducted on the numerical accuracy of the different methods and sampling grid parameters showed that all solutions are numerically similarly accurate at low frequencies, but the binaural output signals differ above the spatial aliasing frequency. The experiment that we present in this article therefore essentially investigates for which parameter set the artifacts due to spatial aliasing are perceptually not relevant. The fact that spatial aliasing occurs only at high frequencies makes the choice of test signal very significant. Many studies in the literature use speech or pulsed pink noise. It is reported in [47] that a pink noise pulse of a duration of 75 ms is a slightly more critical signal in terms of the required SH order of the auralization compared to speech when it comes its influence on the auralization of the direct sound of a room response. Its relatively long stationary part makes it less critical in the auralization of reverberation. The most critical signal that one can conceive is one that is transient and exhibits energy only above the spatial aliasing frequency. As the practical relevance of such a signal is questionable, we choose a 5-second segment of a rock drum rhythm as test signal. It is transient, which makes it suitable to investigate the auralization of reverberation, and it is one of the practically relevant signals that has relatively much energy at high frequencies, which assures that the consequences of spatial aliasing are reflected in the binaural output with sufficient prominence.

The room acoustic conditions that we tested were anechoic and a hall with a reverb decay time of 1 s.

¹<https://mathworks.com>

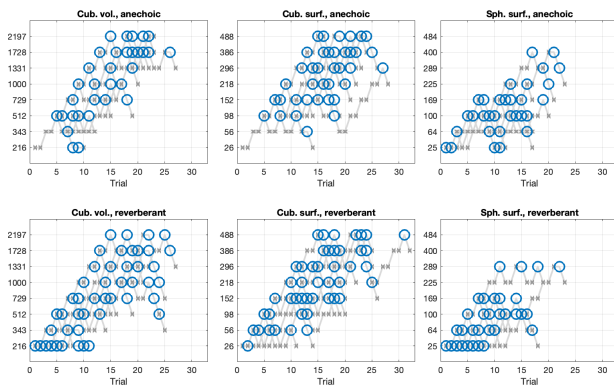
²<https://puredata.info>

³<https://supperware.co.uk>

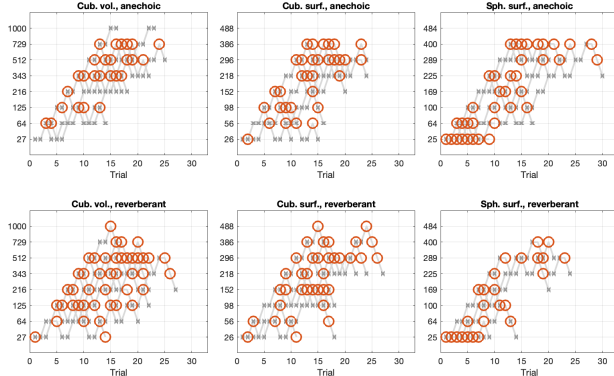
This amounts to a total of $2 \times 3 \times 2 = 12$ (auralization types \times grid shapes \times room types) adaptations that the experiment comprised. Loudness alignment of the stimuli was not necessary as all tested methods preserve the signal level. The playback level was the same for all subjects and was similar to that of conversational speech.

We used the HRTFs from [48] to compute the stimuli. Audio examples of the conditions tested in the present experiment are available at [49].

6 Results and Discussion



(a) Ambisonic auralization



(b) Direct auralization

Figure 6: Adaptation curves for all subjects for ambisonic auralization (a) and direct auralization (b). The red circles mark situations in which the subject did not identify the deviating stimulus correctly. The vertical axis denotes the number of sampling nodes.

16 subjects of different genders with self-reported unimpaired hearing participated in the experiment. All subjects were students or PhD students at the Division of Applied Acoustics at Chalmers University

of Technology. Twelve subjects participated in both sessions that the experiment comprised. The other four participated in only one of the sessions. Data from a total of 14 subjects were therefore available for each of the 12 adaptations. The median duration of the sessions was 30 min; the maximum was 87 min.

We conducted interviews with the subjects directly after each session to obtain additional insights. Most subjects stated that whenever they perceived a difference between a stimulus and the reference, differences were apparent with respect to both spatial impression and timbre. The clearest spatial difference was that some stimuli (presumably the auralization) were perceived closer than others (presumably the ground truth). Most subjects reported that they found it easier to detect differences between stimuli when using the setting where the virtual sound source was on the side.

The subjects' comments suggest that the perceptual distance between the reference and the stimulus does not necessarily decrease monotonically with increasing number of sampling nodes. It is roughly monotonic, but not in a strict sense. The exact parameters of the psychometric function that represents the observed data are therefore not of primary interest (or not even useful to determine) in the present investigation. The main reason is that the present experiment does not investigate an isolated hearing mechanism. Artifacts in the binaural signals may trigger a variety of hearing mechanisms, which may be the cause for the non-monotonic relation between accuracy of the signals and the perceptual distance to the reference. The concept of a psychometric function may therefore not even be applicable.

The main goal of our work is identifying what parameter set makes it highly probable that a human will not perceive any difference between the auralization and the ground truth. We will focus the discussion on this aspect.

The raw responses from the subjects are depicted in Fig. 6, whereby those occasions are marked where the subjects did not identify correctly the stimulus that deviated from the other two stimuli. Major observations are:

- 1) Incorrect responses occurred for almost any number of sampling points. This represents the fact that even comparably low numbers of sampling point can provide auralization that is perceptually close to the ground truth.
- 2) Disregarding clipped adaptations (see below), no subject was able to reliably differentiate stimuli in direct auralization if 1000 pressure sampling nodes for cubical volumetric grids and 386

and 400 double nodes for cubical and spherical surface grids.

- 3) With ambisonic auralization, no subject was able to reliably differentiate stimuli if 2197 pressure sampling nodes for cubical volumetric grids and 386 and 289 double nodes for cubical and spherical surface grids.
- 4) A total of five adaptations for cubical grids clipped meaning that there were subjects who were able to differentiate auralization and ground truth up to the highest number of sampling points that was available.

We emphasize here that the chosen experiment design is very critical in the sense that even the slightest perceptual differences become detectable. The subjects generally considered the task of differentiating the stimuli to be challenging. They stated that once the adaptation had progressed a bit, they many times did not hear a difference between the sounds that they could pinpoint. It was rather such that they had a vague perception that the sounds were not all identical. The subjects that produced the outliers stated this, too.

It was reported in the literature that authentic binaural reproduction of reverberation can be performed at considerably lower SH orders than the direct sound and reverberation were auralized separately. In the present case, where direct sound and reverberation were auralized in the exact same manner, we cannot identify a systematic difference between the subjects’ responses for the reverberant condition compared to the anechoic one. A possible explanation may be that the properties of the direct sound dominate the perception also in the reverberant case. We focus the remaining discussion on the anechoic condition for convenience.

The study that was present in [47] investigated the required SH order for perceptually transparent ambisonic auralization of recordings from rigid spherical microphone arrays, which is a setup that is very similar to the spherical surface grids in our study (Fig. 6a (middle column)). The authors found that the median SH order required was approx. 20, whereas the absolute maximum for any subject was 15 in our case. This difference is most likely do to different choices in the signal processing that were made in [47] compared to present work. We experimented extensively in the preparation of our experiment with different variations of the processing. Many solutions, for example, for equalizing the binaural signals or for performing the required matrix inversion produced auralizations that appeared to be almost perceptually

transparent. Squeezing out that last bit of performance that enabled perceptual transparency was difficult for many of the possible solutions. An important building block in our implementation is the regularized SVD with which we perform the required matrix inversion, which turned out to be clearly preferable in terms of the perceptual result compared to other means of matrix inversion. A similarly regularized SVD was already identified in [51] to provide higher numerical accuracy with respect to a variety of metrics particularly at low frequencies. We confirm that it is preferable also in perceptual terms and provides benefits over the entire frequency range.

[18] also used virtual cardioid sensors for ambisonic auralization of sampled sound fields and confirmed high numerical accuracy of the binaural signals for an SH order of 16. Note that the authors used slightly different signal processing than us, and only data up to a frequency of 10 kHz are shown. Perceptual data are not provided.

A summary of the parameter sets that provide perceptually transparent auralization of sampled sound fields is provided in Tab. 2.

Method \ Grid type	$L_{\text{cub. vol.}}$	$L_{\text{cub. surf.}}$	$L_{\text{sph. surf.}}$
Ambisonic	2197 ⁽¹⁾	488 ⁽²⁾	289
Direct	729 ⁽²⁾	488	400

Table 2: Required number of sampling points for perceptually transparent auralization. The figures for the surface grids represent double nodes. The figure in parentheses denotes the total number (summed over both anechoic and reverberant conditions) of cases in which the adaptation clipped, i.e. cases where perceptual transparency was not achieved for a subject.

At SH orders that are so high that perceptual transparency is achieved, the equalization that we apply in ambisonic auralization is very subtle and potentially inaudible. We chose to apply it by default nevertheless because it can reduce the perceptual distance between ground truth and auralization very much at lower SH orders.

7 Conclusions

Our work showed that the methods for auralization of simulated sound fields that we investigated differ primarily in how spatial aliasing manifests in the binaural output signals. The accuracy of all methods is comparable below the spatial aliasing frequency. The room acoustic conditions that the simulated sound field data represent have no substantial effect on the

requirements for perceptual transparency of the auralization.

We can confirm through extensive experimentation that details of the implementation of the signal processing can be decisive for whether perceptual transparency can be achieved or not. We provide a free implementation of all investigated methods in [27] for reproducibility. It is not inconceivable that further improvements of the signal processing can allow for using even simpler sampling grids.

Surface sampling grids of sound pressure and particle velocity are preferable over volumetric pressure sampling grids because fewer sampling points are required for perceptual transparency. Ambisonic auralization using a spherical surface grid with 289 nodes of sound pressure and particle velocity is the setup that provides perceptual transparency with the lowest number of sampling points. This corresponds to a spherical harmonic order of 15. Direct auralization is less convenient because each desired listener head orientation has to be computed separately. The only condition where direct auralization has a clear perceptual benefit over ambisonic auralization is in combination with volumetric grids.

The requirements for perceptual transparency that we identified have to be considered to be very conservative. The audio examples that we provide demonstrate that perceptually excellent results can be achieved with significantly fewer sampling points.

Our results supercede the ones from [52], which present a similar study but is restricted to volumetric grids and the influence of the auralization procedure on the detectability of numerical dispersion in the simulated sound field.

The spacing of the sampling points when transparent auralization is achieved is approx. 0 mm, which similar to the spacing that, for example, a Cartesian grid in an FDTD simulation over the entire audible bandwidth would exhibit. Interpolation needs to be applied if the simulation grid is not compatible with the desired sampling grid of the auralization. The perceptual implications of this are to be investigated.

The investigated methods have the potential of serving as a universal auralization methods as they can be applied to any acoustic simulation data so long as the data can be converted to a sound pressure and/or particle velocity distribution. The simulation data can originate from a variety of source including geometric acoustics simulations, wave-based simulations, and radiocity. This can make simulation data more straightforward to compare and allows for broadening the scope of round-robin tests like [3]. The code base that accompanies this article provide example projects for auralization data com-

mercial room acoustic simulation softwares with the presented methods.

8 Resources

Implementations of the methods that we investigated in this article are available freely in the Chalmers Auralization Toolbox [27]. Audio examples are available at [49].

References

- [1] M. Vorländer, *Auralization - Fundamentals of Acoustics, Modelling, Simulation, Algorithms and Acoustic Virtual Reality* (Springer, Berlin, Heidelberg, 2008).
- [2] B. N. J. Postma and B. F. G. Katz, “Perceptive and objective evaluation of calibrated room acoustic simulation auralizations,” *The Journal of the Acoustical Society of America*, vol. 140, no. 6, pp. 4326–4337 (2016 12), doi:10.1121/1.4971422.
- [3] F. Brinkmann, L. Aspöck, D. Ackermann, S. Lepa, M. Vorländer, and S. Weinzierl, “A round robin for room acoustical simulation and auralization,” *Journal of the Acoustical Society of America*, vol. 145, no. April, pp. 2746–2760 (2019), doi:10.1121/1.5096178.
- [4] M. Blau, A. Budnik, M. Fallahi, H. Steffens, S. D. Ewert, and S. van de Par, “Toward realistic binaural auralizations – perceptual comparison between measurement and simulation-based auralizations and the real room for a classroom scenario,” *Acta Acust.*, vol. 5, p. 8 (2021), doi:10.1051/aacus/2020034.
- [5] A. Southern, D. T. Murphy, and L. Savioja, “Spatial Encoding of Finite Difference Time Domain Acoustic Models for Auralization,” *IEEE TASLP*, vol. 20, no. 9, pp. 2420–2432 (2012).
- [6] R. Mehra, L. Antani, S. Kim, and D. Manocha, “Source and Listener Directivity for Interactive Wave-Based Sound Propagation,” *IEEE Transactions on Visualization and Computer Graphics*, vol. 20, no. 4 (2014).
- [7] S. Bilbao, A. Politis, and B. Hamilton, “Local Time-Domain Spherical Harmonic Spatial Encoding for Wave-Based Acoustic Simulation,” *IEEE Signal Processing Letters*, vol. 26, no. 4, pp. 617–621 (2019), doi:10.1109/LSP.2019.2902509.

- [8] I. Henderson, A. Politis, and S. Bilbao, “Filter Design for Real-Time Ambisonics Encoding During Wave-based Acoustic Simulations,” presented at the *Forum Acusticum* (2020 Dec.).
- [9] J. A. Hargreaves, L. R. Rendell, and Y. W. Lam, “A framework for auralization of boundary element method simulations including source and receiver directivity,” *JASA*, vol. 145 (2019).
- [10] B. Støfringsdal and P. Svensson, “Conversion of discretely sampled sound field data to auralization formats,” *JAES*, vol. 54, no. 5, pp. 380–400 (2006 may).
- [11] M. A. Poletti and U. P. Svensson, “Beamforming synthesis of binaural responses from computer simulations of acoustic spaces,” *The Journal of the Acoustical Society of America*, vol. 124, no. 1, pp. 301–315 (2008), doi:10.1121/1.2924206.
- [12] J. Sheaffer, M. van Walstijn, B. Rafaely, and K. Kowalczyk, “Binaural Reproduction of Finite Difference Simulations Using Spherical Array Processing,” *IEEE/ACM Transactions on Audio, Speech, and Language Processing*, vol. 23, no. 12, pp. 2125–2135 (2015).
- [13] D. M. Murillo Gómez, J. Astley, and F. M. Fazi, “Low Frequency Interactive Auralization Based on a Plane Wave Expansion,” *Applied Sciences*, vol. 7, no. 6 (2017).
- [14] E. Hulsebos, D. de Vries, and E. Bourdillat, “Improved microphone array configurations for auralization of sound fields by wave-field synthesis,” *JAES*, vol. 50, no. 10, pp. 779–790 (2002 Oct.).
- [15] I. Balmages and B. Rafaely, “Open-Sphere Designs for Spherical Microphone Arrays,” *IEEE TASLP*, vol. 15, no. 2, pp. 727–732 (2007).
- [16] A. J. Burton and G. F. Miller, “The application of integral equation methods to the numerical solution of some exterior boundary-value problems,” *Proc. of the Royal Soc. of London. A.*, vol. 323, no. 1553, pp. 201–210 (1971).
- [17] M. R. P. Thomas, “Practical Concentric Open Sphere Cardioid Microphone Array Design for Higher Order Sound Field Capture,” presented at the *IEEE International Conference on Acoustics, Speech and Signal Processing (ICASSP)*, pp. 666–670 (2019).
- [18] M. Cosnefroy, S. Guðjónsson, and F. Pind, “Physically accurate binaural reproductions from broadband wavebased room acoustics simulations, and comparison with measurements,” presented at the *Immersive and 3D Audio Conference (I3DA)*, pp. 1–8 (2023), doi:10.1109/I3DA57090.2023.10289386.
- [19] T. Pathre, M. Hornikx, and A. Kohlrausch, “Perceptual evaluation of auralizations from a wave-based method in a virtual environment,” presented at the *Euroregio/BNAM*, pp. 105–114 (2022).
- [20] T. Yoshida, , T. Okuzono, and K. Sakagami, “Binaural Auralization of Room Acoustics with a Highly Scalable Wave-Based Acoustics Simulation,” *Applied Sciences*, vol. 13, no. 5 (2023), doi:10.3390/app13052832.
- [21] J. Merimaa and V. Pulkki, “Spatial Impulse Response Rendering I: Analysis and Synthesis,” *Journal of the Audio Engineering Society*, vol. 53, pp. 1115–1127 (2005 Dec.).
- [22] V. Gunnarsson and M. Sternad, “Binaural Auralization of Microphone Array Room Impulse Responses Using Causal Wiener Filtering,” *IEEE/ACM Transactions on Audio, Speech, and Language Processing*, vol. 29, pp. 2899–2914 (2021), doi:10.1109/TASLP.2021.3110340.
- [23] V. Pulkki, “Spatial sound reproduction with directional audio coding,” *Journal of the Audio Engineering Society*, vol. 55, pp. 503–516 (2007 Jun.).
- [24] A. Politis, S. Tervo, and V. Pulkki, “COMPASS: Coding and Multidirectional Parameterization of Ambisonic Sound Scenes,” presented at the *IEEE International Conference on Acoustics, Speech and Signal Processing (ICASSP)*, pp. 6802–6806 (2018), doi:10.1109/ICASSP.2018.8462608.
- [25] F. Zotter and M. Frank, *Ambisonics: A Practical 3D Audio Theory for Recording, Studio Production, Sound Reinforcement, and Virtual Reality* (Springer, Heidelberg, 2019).
- [26] J. Ahrens, “A Software Tool for Auralization of Simulated Sound Fields,” presented at the *Proc. of the Institute of Acoustics*, vol. 45(2) (2023 Sep.).
- [27] J. Ahrens, “The Chalmers Auralization Toolbox,” <https://github.com/AppliedAcousticsChalmers/auralization-toolbox> (2024), (last visited on 2024-10-31).

- [28] M. X. Cohen, *Linear Algebra: Theory, Intuition, Code* (sincXpress, 2021).
- [29] N. Gumerov and R. Duraiswami, *Fast Multipole Methods for the Helmholtz Equation in Three Dimensions* (Elsevier, Amsterdam, 2005).
- [30] E. Williams, *Fourier Acoustics: Sound Radiation and Nearfield Acoustical Holography* (Academic Press, New York, 1999).
- [31] J. Ahrens, “How small can a baffled ambisonic microphone array be?” presented at the *Proc. of DAGA* (2024 Mar.).
- [32] C. Schörkhuber, M. Zaunschirm, and R. Höldrich, “Binaural Rendering of Ambisonic Signals via Magnitude Least Squares,” presented at the *Proceedings of DAGA*, pp. 339–342 (2018 Mar.).
- [33] J. Ahrens, “Binaural Audio Rendering in the Spherical Harmonic Domain: A Summary of the Mathematics and Its Pitfalls,” Technical note v. 2, Chalmers University of Technology (2022).
- [34] T. Deppisch, H. Helmholtz, and J. Ahrens, “End-to-End Magnitude Least Squares Binaural Rendering of Spherical Microphone Array Signals,” presented at the *Immersive and 3D Audio: from Architecture to Automotive (I3DA)*, pp. 1–7 (2021), doi:10.1109/I3DA48870.2021.9610864.
- [35] G. Chardon, W. Kreuzer, and M. Noisternig, “Design of Spatial Microphone Arrays for Sound Field Interpolation,” *IEEE Journal of Selected Topics in Signal Processing*, vol. 9, pp. 780–790 (2015), doi:10.1109/JSTSP.2015.2412097.
- [36] S. Koyama, Gilles, Chardon, and L. Daudet, “Optimizing Source and Sensor Placement for Sound Field Control: An Overview,” *IEEE/ACM Trans. on Audio, Speech, and Language Processing*, vol. 28, pp. 696–714 (2020), doi:10.1109/TASLP.2020.2964958.
- [37] S. A. Verburg, F. Elvander, T. van Waterschoot, and E. Fernandez-Grande, “Optimal sensor placement for the spatial reconstruction of sound fields,” *Journ. on Audio, Speech, and Music Proc.*, vol. 41 (2024), doi:10.1186/s13636-024-00364-4.
- [38] J. Fliege and U. Maier, “The distribution of points on the sphere and corresponding cubature formulae,” *IMA Journal of Numerical Analysis*, vol. 19, no. 2, pp. 317–334 (1999), doi:10.1093/imanum/19.2.317.
- [39] S. Tervo, J. Pätynen, A. Kuusinen, and T. Lokki, “Spatial decomposition method for room impulse responses,” *Journal of the Audio Engineering Society*, vol. 61, pp. 17–28 (2013 Dec.).
- [40] N. Kaplanis, “Perception of Reverberation in Domestic and Automotive Environments,” PhD thesis, Aalborg Universitet (2017).
- [41] J. Ahrens, “Perceptual Evaluation of Binaural Auralization of Data Obtained from the Spatial Decomposition Method,” presented at the *IEEE Workshop on Applications of Signal Processing to Audio and Acoustics (WASPAA)*, pp. 65–69 (2019), doi:10.1109/WASPAA.2019.8937247.
- [42] J. Ahrens, “Acoustic Room Responses,” <https://github.com/AppliedAcousticsChalmers/acoustic-room-responses> (2024), (last visited on 2024-10-31).
- [43] H. Levitt, “Transformed Up-Down Methods in Psychoacoustics,” *The Journal of the Acoustical Society of America*, vol. 49, no. 2B, pp. 467–477 (1971 02), doi:10.1121/1.1912375.
- [44] M. Geier, J. Ahrens, and S. Spors, “The Sound-Scape Renderer: A Unified Spatial Audio Reproduction Framework for Arbitrary Rendering Methods,” presented at the *124th Conv. of the AES* (2008 May).
- [45] M. Zaunschirm, C. Schörkhuber, and R. Höldrich, “Binaural rendering of Ambisonic signals by head-related impulse response time alignment and a diffuseness constraint,” *The Journal of the Acoustical Society of America*, vol. 143, no. 6, pp. 3616–3627 (2018 06), doi:10.1121/1.5040489.
- [46] J. Ahrens and C. Andersson, “Perceptual evaluation of headphone auralization of rooms captured with spherical microphone arrays with respect to spaciousness and timbre,” *Journal of the Acoustical Society of America*, vol. 145, no. April, pp. 2783–2794 (2019), doi:10.1121/1.5096164.
- [47] T. Lübeck, J. M. Arend, and C. Pörschmann, “Binaural reproduction of dummy head and spherical microphone array data—A perceptual study on the minimum required spatial resolution,” *The Journal of the Acoustical Society of America*, vol. 151, no. 1, pp. 467–483 (2022 01), doi:10.1121/10.0009277.
- [48] B. Bernschütz, “A Spherical Far Field HRIR/HRTF Compilation of the Neumann KU 100,” presented at the *Proceedings of AIA/DAGA*, pp. 592–595 (2013 Mar.).

- [49] J. Ahrens, “Audio examples for ‘Perceptually Transparent Binaural Auralization of Simulated Sound Fields’,” <http://www.ta.chalmers.se/research/audio-technology-group/audio-examples/jaes-2024b/> (2024), (last visited on 2024-10-31).
- [50] I. Engel, C. Henry, S. V. Amengual Garí, P. W. Robinson, and L. Picinali, “Perceptual implications of different Ambisonics-based methods for binaural reverberation,” *The Journal of the Acoustical Society of America*, vol. 149, no. 2, pp. 895–910 (2021 02), doi:10.1121/10.0003437.
- [51] A. Politis and H. Gamper, “Comparing modeled and measurement-based spherical harmonic encoding filters for spherical microphone arrays,” presented at the *IEEE Workshop on Applications of Signal Processing to Audio and Acoustics (WASPAA)*, pp. 224–228 (2017), doi:10.1109/WASPAA.2017.8170028.
- [52] J. Meyer, T. Lokki, and J. Ahrens, “Identification of Virtual Receiver Array Geometries that Minimize Audibility of Numerical Dispersion in Binaural Auralizations of Finite Difference Time Domain Simulations,” presented at the *Proc. of the 149th Convention of the AES* (2020 Oct.).